2025 IEEE/SICE International Symposium on System Integration (SII)
January 21-24, 2025, Munich, Germany

Development of an automated method for extracting reflectance maps of road marking areas by camera-LiDAR fusion*

Akisue Kuramoto, Ryo Yanase, Keisuke Yoneda and Naoki Suganuma

Abstract— **A system that can automatically determine where and when the prior knowledge map needs to be updated according to the new observation would be helpful in avoiding poor accuracy and reliability of map matching for self-position estimation. Such a system is also useful for road maintenance and management to identify areas where repainting work is required. Therefore, as a first effort to develop such a system, this paper proposes a lidar-camera fusion framework to extract road marking areas from reflectance maps for quantifying the reflectance of the areas, which can be detected and confirmed using camera images.**

I. Introduction

Digital maps, including road markings, road shape information, lane-level directed graphs, traffic light position information, etc., are essential for autonomous driving systems for public roads to drive harmoniously with traffic participants. In our previous research, LiDAR reflectance maps have been used as digital maps considering both road markings and the surrounding environment in map matching for self-localization [1]-[5]. However, the position and condition of actual road markings can change suddenly or gradually. For example, due to road construction or other factors, the actual position of road markings may change to a different position from that of the digital map generated based on past data (hereafter, the prior knowledge map). It is strongly recommended to repaint road markings every 9 to 12 months [6] because there are many situations where they are gradually degraded and are almost faded. Furthermore, some general roads do not even have white lines. In these scenes, the LiDAR reflectance of the road markings is low, which tends to reduce the accuracy and reliability of map matching for self-location estimation [7]. To avoid this problem, it would be ideal to keep the prior knowledge map up to date [7], but this is not easy because it requires continuously maintaining the latest data covering the entire digital map.

A system that can automatically determine where and when the prior knowledge map needs to be updated according to the new observation would be helpful in avoiding poor accuracy and reliability of map matching for self-position estimation. Such a system is also useful for road maintenance and management to identify areas where repainting work is required. One approach for building such system is to develop an algorithm to determine whether road markings have degraded from road marking maps based on a 3D point cloud containing reflectance data. Such point cloud can be obtained by simultaneous observations of LiDAR and GNSS/IMU systems. For example, Iparraguirre et al. proposed a method to input a digital map using a deep learning architecture to determine whether road markings have degraded [8]. However, this method has a problem in that it is difficult to evaluate the degree of degradation of road markings. Soilán et al. proposed a method to automatically extract areas where road markings have deteriorated, using a regression equation that estimates retroreflective performance (reflectance obtained by a reflectance meter) using LiDAR reflectance as a variable [9]. However, this method requires manual setting of a threshold value for LiDAR reflectance when extracting a point cloud of the road marking area to derive the regression equation.

Many classic studies have proposed image-processing methods for recognizing road markings by pattern recognition or semantic segmentation on onboard camera image. However, these methods have difficulty in considering the reflectance of road markings.

In this paper, as a first effort towards developing a fully automatic system for determining the deterioration state of road markings, we propose a fully automatic framework that extracts reflectance data only in the road marking area by fusing LiDAR, cameras, and GNSS/IMU systems.

II. Proposed Method

Figure 1 shows an overview of the proposed method procedures. At each data time, semantic segmentation is first applied to the onboard camera image, as shown in Fig. 1(a), to obtain probability value of road marking at each pixel. Next, from the LiDAR observation point cloud, only points that can be projected onto pixels with a high probability of road marking are extracted. Using the extracted points, an orthogonal map of road marking probability is generated as shown in Fig. 1(b). At the same time, an orthogonal map based on the 3D coordinates and reflectance data of the LiDAR point cloud is also generated as shown in Fig. 1(c). The orthogonal map of road marking probability (Fig. 1(b)) is binarized with a threshold value, which is set automatically by discriminant analysis, and areas that are more likely to be road markings than the surrounding areas are extracted as shown in Fig. 1(d). This binarized image is applied as a mask image to the reflectance orthogonal maps (Fig. 1(c)) for extracting reflectance data on only areas with a high probability of road markings (Fig. 1(f)). The number of pixels with non-zero reflectance in Fig. 1(f) and the average reflectance of only the non-zero pixels are expected to be

*Resrach supported by Suzuki Foundation.

A. Kuramoto is with Institute of Science Tokyo (Tokyo Institute of Technology), Meguro, Tokyo 1528550 Japan (corresponding author to provide phone: +81-3-5734-2641; e-mail: akisuekura@sc.e.titech.ac.jp).

R. Yanase, K. Yoneda and N. Suganuma, were with Kanazawa University, Kanazawa, Ishikawa 9201192 Japan. They are now with the Advanced Mobility Research Institute, Kanazawa University. (ryanase@staff.kanazawa-u.ac.jp / k.yoneda@staff.kanazawa-u.ac.jp / suganuma@staff.kanazawa-u.ac.jp)

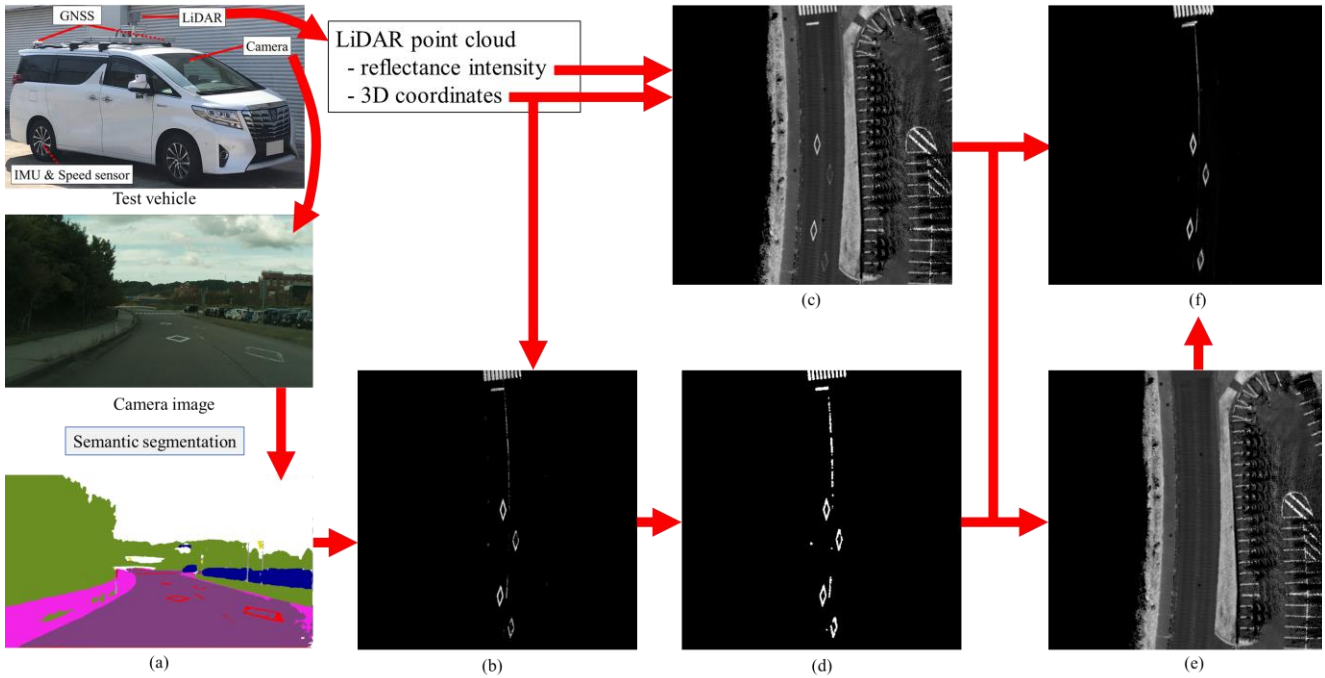

Fig. 1 Overview of the procedure of the proposed method. (a) Semantic segmentation result. (b) Probability map of road markings. (c) LiDAR intensity map around the test vehicle. (d) Binarized image of the probability map of road markings. (e) Reflectance map that masked areas with a high probability of road markings by the average reflectance values of asphalt area. (f) LiDAR intensity map only for areas that are likely to be road markings.

potential indicators of deterioration of the road markings near this location.

III. Data Collection

Data collection was performed using a test vehicle owned by Kanazawa University. The test vehicle was equipped with a LIDAR VLS-128-AP, an Applanix PosLV 220, and a forward-looking SONY IMX390 camera. The sampling rates of each sensor were 100 Hz, 100 Hz, and 10 Hz, respectively. The position and attitude of the vehicle at each time were obtained from GNSS-RTK data after post-processing correction.

Data collection was carried out by manually driving through areas where data collection had been conducted previously among the areas where road markings were repainted in 2023. Information on the areas where road markings were repainted was provided by the Civil Engineering Central Office, Ishikawa Prefecture. On October 23, 2023, the weather was sunny with occasional clouds, and the road surface was dry. In data processing, only data in which the vehicle was traveling at a speed of 5km or more at the time of camera capture was extracted and analyzed.

IV. Results and Discussion

The series of Figure 2 show examples of orthogonal maps created using the proposed method explained in Chapter 2. Pixel coordinates of both maps were determined by post-processed vehicle position recorded by a GNSS-RTK system. Each pixel value in Fig. 2(a) indicates the LiDAR reflectance at that position. It is shown that not only road markings but also sidewalks and plants area return relatively high reflectance. The LiDAR reflectance of dotted center lines is not significantly higher than that of the surroundings. Each pixel value in Fig. 2(b) indicates the probability of the road marking in each pixel position. Crosswalks and diamond-shaped markings are estimated to have a high probability, and they are clearer than in LiDAR reflectance map. The dotted center lines area has also higher probability than the surrounding area and this gives clearer impression than in the LiDAR reflectance image.

In the parking lot area on the right side of the maps, some division lines can be seen in Fig. 2(a), but not in Fig. 2(b). This is because the area to which semantic segmentation can be applied is limited to the viewing angle range of the in-vehicle camera, and because parked vehicles block the lane markings on the camera image.

Figure 3 shows the distribution of the number of pixels of road markings and the average of LiDAR reflectance intensity at those pixels. There was a weak correlation (R=0.30) between the number of pixels determined to be road markings and the average LiDAR reflectance intensity.

Figure 4 to Figure 6 show some characteristic scenes. Figure 4 shows an example in the scene both the number of pixels of road markings and the average of LiDAR reflectance intensity are high. Most of road markings are very clear in camera image (Fig. 4(a)) and LiDAR reflectance intensity map around ego vehicle (Fig. 4(b)). The LiDAR intensity map of only areas that are likely to be road markings (Fig. 4(c)) suggest that road markings that can be detected on the camera image have high LiDAR reflection intensity. Also, comparing Figure 4 (b) and (c), the LiDAR reflection intensity in the area around the road is middle. These results suggest that the contribution of the road markings to self-localization using ZNCC-based map matching at this point is high in this scene [5].

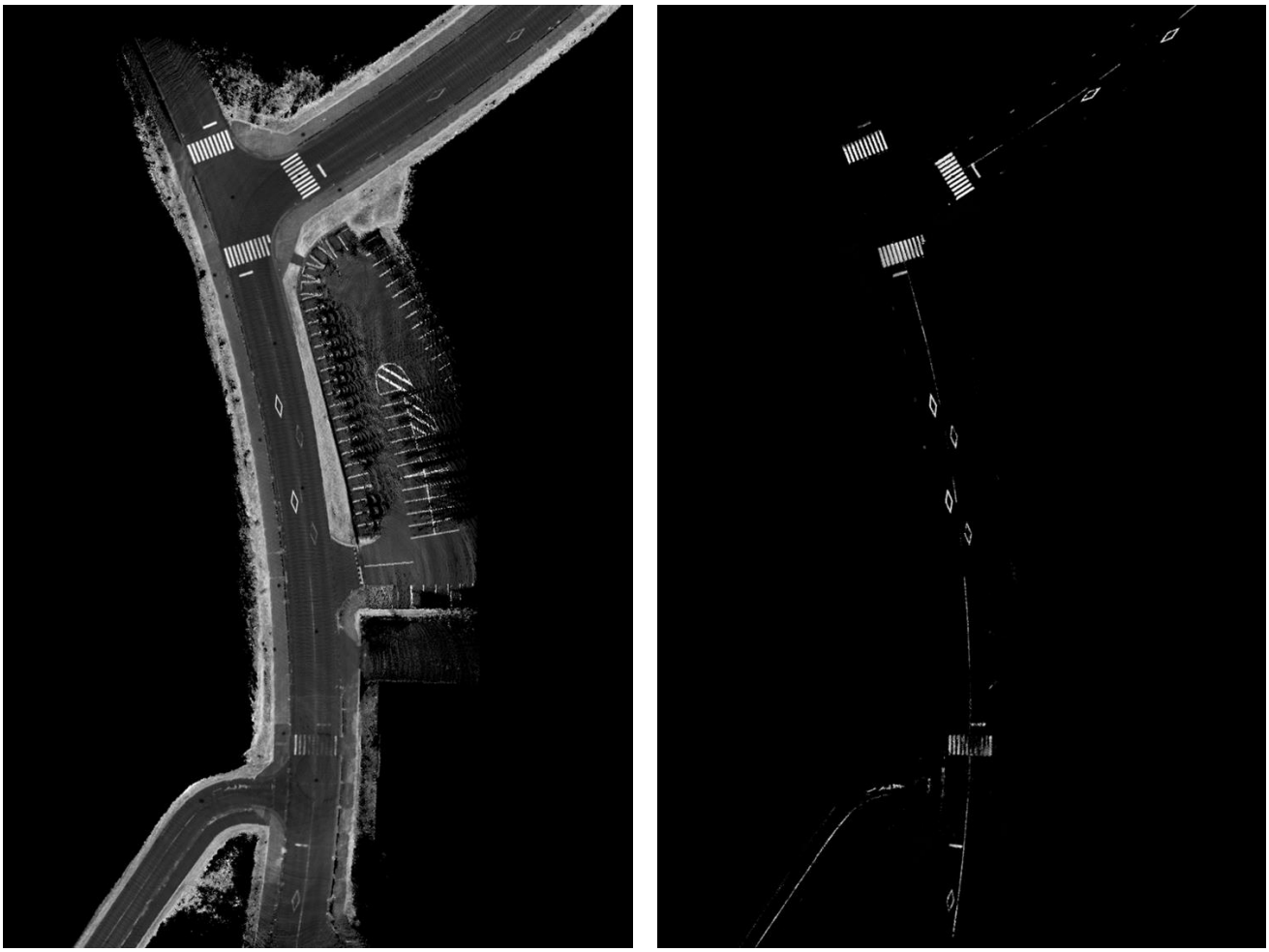

(a) pixel value: LiDAR reflectance

(b) pixel value: probability of road mark estimated by semantic-segmentation method

Fig. 2 Examples of created orthogonal maps. Pixel coodinates of both maps were determined by post-processed vehicle position recorded by a GNSS-RTK system.

Figure 5 shows an example of a scene with a small number of road marking pixels but a high average LiDAR reflection intensity. In this scene, the camera image shows that while the white line on the roadside strip is almost invisible, the center dotted line is very clear (Fig. 5(a)). This center dotted line is very clear in both LiDAR reflection intensity map around ego vehicle (Fig. 5(b)) and LiDAR reflection intensity map of only the areas that are likely to be road markings (Fig. 5(c)). These results indicate that the dotted line detectable on the camera image has high LiDAR reflection intensity. On the other hand, the fact that the white lines on the roadside strips have almost disappeared caused the number of pixels in the road markings to be small. This result suggests that the number of pixels in road markings may be one of effective indicators for evaluating the degree of deterioration of white lines.

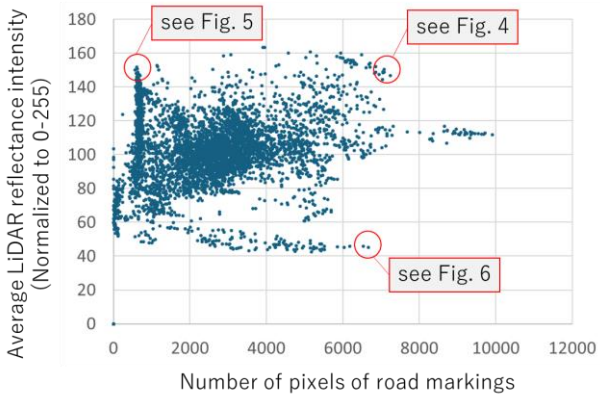

Fig. 3 Distribution of the number of pixels of road markings and the average of LiDAR reflectance intensity at those pixels.

Figure 6 shows an example of a scene with a high number of road marking pixels but a low average LiDAR reflection intensity. This scene was recorded inside a tunnel where the lanes are being repainted in near future. In the camera image, the white line of the roadside strip is visible, but the center line has almost disappeared (Fig. 6(a)). However, LiDAR reflection intensity map around ego vehicle (Fig. 6(b)) shows that reflectance of road markings are very low not only on the center line has almost disappeared, but also on the white line on the roadside strip. A LiDAR intensity map of only the area that appears to be a road marking (Fig. 6(c)) shows that it was able to detect the white line of the roadside strip on the camera image. From these facts, the LiDAR reflectance intensity of the white line detected on the camera image is low. These results suggest that the average LiDAR reflectance intensity number of pixels in road markings may be one of effective

indicators for evaluating the degree of deterioration of road markings. These results also suggest that it would be better to repaint the white line on the roadside strip, as well as the center line, which has almost disappeared.

To examine whether it is possible to automatically classify between these characteristic degradation states, we tried a series of unsupervised learning methods. As a preparation, we defined a state vector of road markings around the test vehicle at each point, $\boldsymbol{s} = \{s_1, s_2, s_3, s_4, s_5, s_6, s_7\}$, where each component is described in Table1. Then, the series of $\boldsymbol{s}$ was calculated for the locations at each second among the recorded driving data. The series of $\boldsymbol{s}$ was first classified using a one-class SVM using RBF kernels to determine whether it can be considered average within the driving area. The parameter υ (nu) in the one-class SVM was set to 0.33. After that, the series of $\boldsymbol{s}$ that were determined to be not average were classified into three types using the k-menas algorithm.

Table1. Elements and its descriptions of the state vector of road markings

Element	Description
s_1	Number of pixels of road markings
s_2	Average reflectance on road markings
s_3	Standard deviation of reflectance on road markings
s_4	Average reflectance on asphalt around road markings
s_5	Standard deviation of reflectance on asphalt around road markings
s_6	Reflectance difference $(= s_2 - s_4)$
s_7	Reflectance ratio $(= s_2/s_4)$

Figure 7 shows the classification results of the state vectors of road markings $\boldsymbol{s}$. Colors indicate each class: normal or anomaly classes 1 to 3. The anomaly class 1 consist of locations judged to be non-average but difficult to distinguish from the average point. This class included the location where the scene both the number of pixels of road markings and the average of LiDAR reflectance intensity are high like shown in Fig.4. The anomaly class 2 seems to consist of locations with a small number of road marking pixels but a high average LiDAR reflection intensity like shown in Fig.5. The anomaly class 3 seems to consist of locations with a high number of road marking pixels but a low average LiDAR reflection intensity like shown in Fig.6.

In this study, we subjectively set a hyperparameters, that is υ (nu) in the one-class SVM to 0.33 and the number of classes on the abnormal side to 3 in the k-means clustering. To verify the validity of the υ, we again classified all $\boldsymbol{s}$ into two classes using k-means method, and it resulted in a 1:2 classification. This result suggests that even with the k-means method, 1/3 of the data can be dissimilar to the remaining 2/3. Although the classification results using the k-means method and OCSVM do not match completely, it is indicated that the nu used in this study was reasonable. The number of classes on the abnormal side in the k-means clustering was set to 3 subjectively in this study. This setting is based on subjective impressions and is a challenge for fully automating the method. However, many algorithms have already been proposed to automatically set the number of clusters, such as the x-means method [10]. By using those methods, it is expected that the proposed system will be able to quantitatively evaluate and detect the degradation state of road marking areas through fully automated procedures.

V. CONCLUSION

In this paper, we proposed a lidar-camera fusion framework that can extract road marking regions from reflectance maps, quantify the reflectance of the regions, and detect and confirm them using camera images.

The proposed method showed a weak correlation between the number of pixels determined as road markings and the average reflection intensity of LiDAR. In addition, it was suggested that the indicators obtained by the proposed method could be useful in suggesting repainting of road markings in some characteristic scenes.

The proposed method has some limitations. First, it may be difficult to apply this method when urban roads are congested and there are many vehicles on the lanes. This is caused by limited field of view of onboard camera used in the data collection in this study. A fish-eye camera may be helpful to avoid this limitation. Second, it is not easy to detect road markings that have almost disappeared in camera images. However, it is expected that this problem can be avoided by using the proposed method to suggest repainting before it disappears. Finally, the criterion for suggesting repaints need to be defined in the future. At present, we are only evaluating the results somewhat qualitatively. It is necessary to discuss what kind of deterioration of road markings is critical to self-position estimation results.

REFERENCES

[1] M. Aldibaja, N. Suganuma, and K. Yoneda, "2.5D Layered Sub-Image LIDAR Maps for Autonomous Driving in Multilevel Environments," Remote Sens, vol. 14, no. 22, 2022, Paper ID: 5847.

[2] A. Kuramoto, M. Aldibaja, R. Yanase, J. Kameyama, K. Yoneda, and N. Suganuma, "Mono-camera based 3D object tracking strategy for autonomous vehicles," 2018 IEEE Intelligent Vehicles Symposium (IV), 2018, pp. 459-464.

[3] K. Yoneda, A. Kuramoto, N. Suganuma, T. Asaka, M. Aldibaja, and R. Yanase, "Robust traffic light and arrow detection using digital map with spatial prior information for automated driving," Sensors, vol. 20, no. 4, 2020, Paper ID; 1181.

[4] K. Yoneda, N. Hashimoto, R. Yanase, M. Aldibaja and N. Suganuma, "Vehicle localization using 76GHz omnidirectional millimeter-wave radar for winter automated driving," in *Proc. 2018 IEEE Intelligent Vehicles Symposium (IV)*, 2018, pp. 971-977.

[5] A. Kuramoto, J. Kameyama, R. Yanase, M. Aldibaja, K. Yoneda and N. Suganuma, "Digital map based signal state recognition of fat traffic lights with low brightness," in *Proc. IECON 2018-44th Annual Conference of the IEEE Industrial Electronics Society*, 2018, pp. 5445-5450.

[6] Japan Road Sign and Marking Association, "Road Marking Handbook: 5th Edition," 2018, p.39 (in Japanese)

[7] A. Kuramoto, H. Kawanishi, R. Yanase, K. Yoneda, and N. Sugnuma, "Effect of road markings wear on accuracy of ZNCC-based map matching," International Journal of Autonotive Engineering, vol. 14, no. 1, 2023, pp. 20-26.

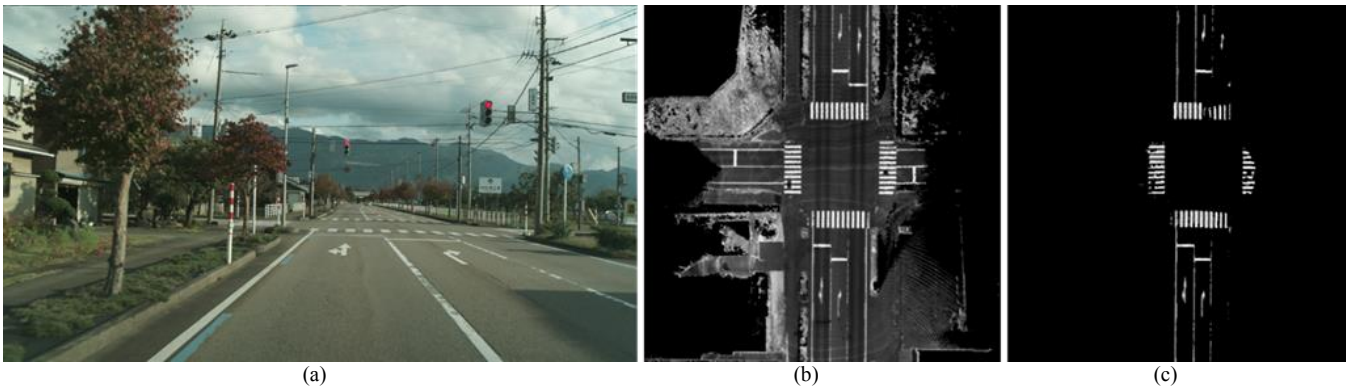

(a) (b) (c)

Fig. 4 An example in the scene with large number of pixels of road markings and high average of LiDAR reflectance intensity. (a) camera image. (b) LiDAR reflectance intensity map around ego vehicle, and (c) LiDAR intensity map only for areas likely to be road markings.

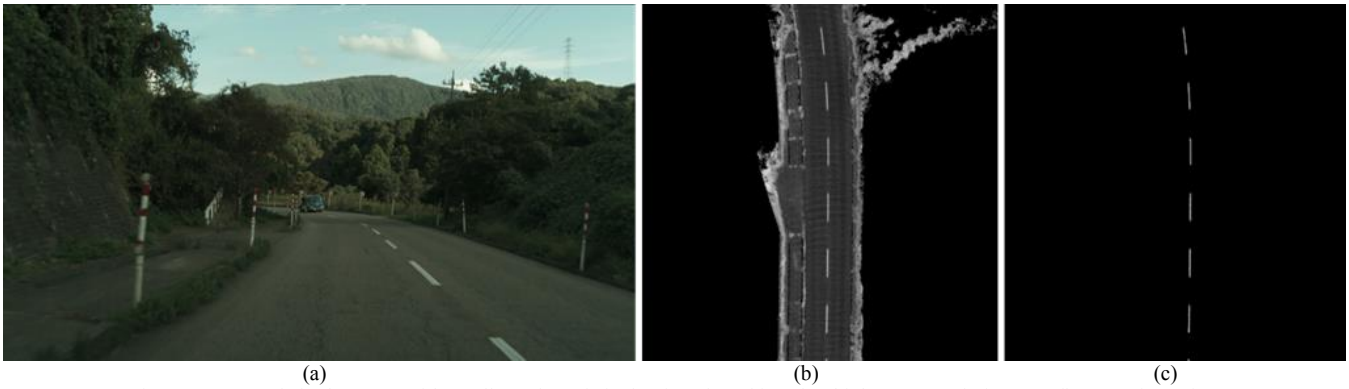

(a) (b) (c)

Fig. 5 An example in the scene with small number of pixels of road markings but high average of LiDAR reflectance intensity. (a) camera image. (b) LiDAR reflectance intensity map around ego vehicle, and (c) LiDAR intensity map only for areas likely to be road markings.

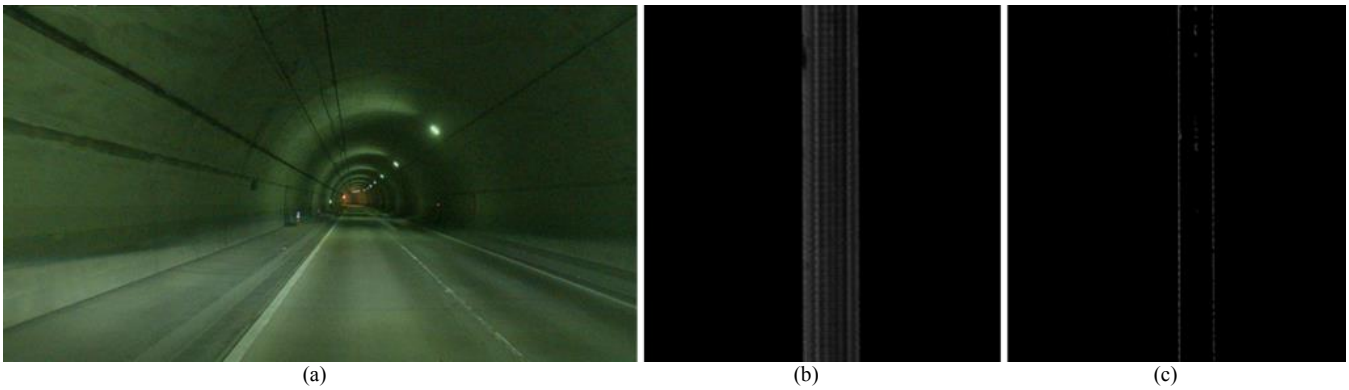

(a) (b) (c)

Fig. 6 An example in the scene with small number of pixels of road markings and low average of LiDAR reflectance intensity. (a) camera image. (b) LiDAR reflectance intensity map around ego vehicle, and (c) LiDAR intensity map only for areas likely to be road markings.

[8] O. Iparraguirre, N. Iturbe-Olleta, A. Brazalez, and D. Borro, “Road marking damage detection based on deep learning for infrastructure evaluation in emerging autonomous driving,”. *IEEE Trans. Intelligent Transportation Systems*, vol. 23, no. 11, 2022, pp. 22378-22385.

[9] M. Soilán, D. González-Aguilera, A.del-Campo-Sánchez, D. Hernández-López and S.Del Pozo, “Road marking degradation analysis using 3D point cloud data acquired with a low-cost Mobile Mapping System,” Automation in Construction, vol. 141, 2022, pp. 104446.

[10] D. Pelleg and A. Moore. "X-means: Extending K-means with E cient Estimation of the Number of Clusters." *ICML'00*. 2000, pp. 727-734.

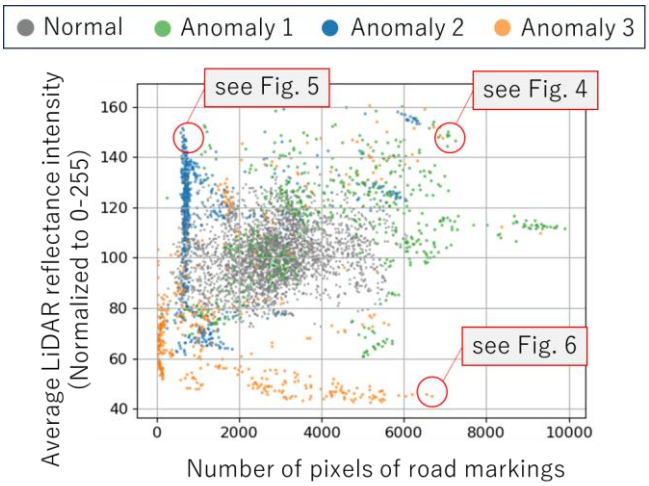

Fig. 7 Classification results of the state vectors of road markings. Colors indicate each class; normal or anomaly classes 1 to 3.